Biochemical and Biophysical Research Communications 434 (2013) 394–400

Contents lists available at SciVerse ScienceDirect

Biochemical and Biophysical Research Communications

journal homepage: www.elsevier.com/locate/ybbrc

High glucose-induced apoptosis in cultured podocytes involves TRPC6-dependent calcium entry via the RhoA/ROCK pathway

He Yang, Bo Zhao, Chang Liao, Rui Zhang, Kexin Meng, Jia Xu, Jundong Jiao *

Department of Nephrology, The Second Affiliated Hospital, Harbin Medical University, PR China

ARTICLE INFO

Article history:
Received 27 March 2013
Available online 6 April 2013

Keywords:
TRPC6
Podocytes
ROS
RhoA GTPase
Apoptosis

ABSTRACT

Increasing evidence indicates that podocyte apoptosis is a key event in the development of diabetic nephrology. However, the underlying mechanism of this apoptosis remains poorly understood. In this study, we report that high levels of glucose enhanced the expression of TRPC6 and TRPC6-dependent Ca^{2+} influx, but glucose levels did not affect TRPC1 and TRPC5 expression. TRPC6 knockdown by siRNA interference attenuated the observed increase in glucose-induced podocyte apoptosis. High glucose levels also increased the generation of ROS; inhibition of ROS activity by N-acetyl-L-cysteine attenuated the high glucose-induced increase in TRPC6 expression and Ca^{2+} influx. Exogenous treatment with H_2O_2 mimicked the high glucose response, resulting in an increase in TRPC6 expression and Ca^{2+} influx. Taken together, these data suggest that high glucose levels induce ROS, thereby mediating TRPC6 expression and Ca^{2+} influx. Because RhoA activity is increased following TRPC6 activation, we investigated whether TRPC6 is involved in high glucose-induced apoptosis via the RhoA/ROCK pathway. We report that high glucose levels produced an increase in RhoA activity, and this effect was abolished by the knockdown of TRPC6. Moreover, inhibition of the RhoA/ROCK pathway by a ROCK inhibitor, Y27632, also attenuated high glucose-induced apoptosis. We conclude that TRPC6 is involved in high glucose-induced podocyte apoptosis through the RhoA/ROCK pathway.

1. Introduction

Considerable evidence suggests that podocyte apoptosis is a key event in the development of diabetic nephropathy (DN) [1–4]. Morphometric analyses of renal biopsy samples indicate that the density of podocytes is reduced in individuals with DN and in patients with a short duration of diabetes before the onset of microalbuminuria [1]. Moreover, a decreased number of podocytes per glomeruli is the strongest predictor of the progression of DN; fewer podocyte cells predict a more rapid disease progression [1,2]. Several lines of evidence indicate that podocyte apoptosis contributes to this reduced podocyte number [3–5]. However, the mechanisms that underlie podocyte apoptosis, in particular, as induced by high levels of glucose, remain poorly understood.

Podocytes are non-excitable cells that lack voltage-gated calcium channels but express a family of non-selective cation channels termed transient receptor potential canonical channels (TRPC) that may contribute to calcium influx [6]. TRPC1, TRPC5, and TRPC6 have been identified in podocytes [7]. Within the TRP channel family, TRPC6 is tightly linked to hereditary and acquired forms of proteinuric kidney diseases [7,8]. TRPC6 channels typically function as downstream components of phospholipase C signaling cascades that liberate diacylglycerol (DAG) and inositol 1,4,5-trisphosphate (IP_3) [6]. TRPC6 is not activated by IP_3 in heterologous systems, but it can be directly activated by DAG; this process is referred to as a receptor-operated calcium entry (ROCE) [6,9]. TRPC1 and TRPC5 can be activated by Ca^{2+} mobilization from intracellular stores mediated by IP_3 or thapsigargin (TG); this process is referred to as a store-operated calcium entry (SOCE) [6,10]. TRPC6 can also be activated by reactive oxygen species (ROS), which results in the trafficking of TRPC6 to the cell surface [11,12]. One significant consequence of TRPC6 activation in podocytes is an increase in RhoA activity [13]. RhoA is a small GTPase that interacts with a downstream effector, Rho-associated coiled coil-containing protein kinase (ROCK), to control many cellular processes, including apoptosis [5,13,14]. Recent investigations demonstrate that the induction of activated RhoA in a podocyte-specific manner results in proteinuria and podocyte apoptosis [15,16]. Moreover, the sustained activation of TRPC6 mediates podocyte apoptosis induced by angiotensin II treatment [17], albumin overload [18], and activation of N-methyl-D-aspartate (NMDA) receptors [11].

We hypothesize that a TRPC6-dependent Ca^{2+} influx contributes to podocyte apoptosis induced by high glucose levels. In this study, we examine the effects of high glucose levels on TRPC6 expression and the potential link with the mediation of podocyte apoptosis.

* Corresponding author. Address: Xuefu Road 246, Harbin 150081, PR China.
E-mail address: jiaojundong@yahoo.com.cn (J. Jiao).

0006-291X/$ - see front matter © 2013 Elsevier Inc. All rights reserved.
http://dx.doi.org/10.1016/j.bbrc.2013.03.087

2. Materials and methods

2.1. Cell culture and plasmid transfection

Conditionally immortalized human podocytes were cultured as previously described [19]. In brief, the cells were grown at 33 °C in RPMI-1640 medium (HyClone, USA), supplemented with ITS (insulin, transferrin, sodium selenate; Sigma, USA) and 10% FBS (HyClone, USA). To induce differentiation, the podocytes were cultured at 37 °C in the same medium for 11–14 days. The cells were transiently transfected with TRPC6 siRNA (sc-42672; Santa Cruz, USA) using the X-treme GENE siRNA transfection reagent (Roche, Germany) according to the manufacturer's instruction. The transfected cells were assayed 24–48 h post-transfection.

2.2. Quantitative real-time PCR

RT-PCR was performed using standard methods as described previously [20]. The primer sequences used to amplify TRPC1, TRPC5 and TRPC6 were as follows (5′-3′): TRPC1 sense CGCCGAACGAGGTGAT and TRPC1 antisense GCACGCCAGCAAGAAA; TRPC5 sense CCACCAGCTATCAGATAAGG and TRPC5 antisense CGAAAGAAGCCACTTATACC; and TRPC6 sense GCCAATGAGCATCTGGAAAT and TRPC6 antisense TGGAGTCACATCATGGGAGA. GAPDH was used as an internal control, and $\Delta\Delta Ct$ was calculated for each sample with the expression levels indicated by values of $2^{-\Delta\Delta Ct}$.

2.3. Western blotting

Western blots were performed using a standard protocol as described previously [20] and probed with the following primary antibodies: polyclonal rabbit anti-TRPC1, -TRPC5, or -TRPC6 antibodies (Alomone Labs, Israel) or an anti-actin antibody (Santa Cruz, USA). The membranes were washed extensively and incubated with fluorescence-conjugated goat anti-rabbit or goat anti-mouse IgG secondary antibodies (Invitrogen, USA). Western blot bands were quantified using the Odyssey infrared imaging system (Li-COR Bioscience, USA).

2.4. Fluorescence measurement of $[Ca^{2+}]i$

$[Ca^{2+}]i$ levels were measured as described previously [20]. Briefly, the podocytes were grown on coverslips and treated with 1% physiological saline solution containing Fluo-3/AM (3 μM, Molecular Probes, USA) and Pluronic F-127 (0.03%, Sigma, USA) for 45 min at 37 °C. The fluorescence intensity of Fluo-3 in the podocytes was recorded using a laser scanning confocal microscope (FV300; Olympus, Japan). The $[Ca^{2+}]i$ was expressed as a pseudo-ratio value of the actual fluorescence intensity divided by the average baseline fluorescence intensity. Calibrations were performed immediately following each experiment. Data from 20 to 40 cells were compiled from a single run, and at least three independent experiments were conducted.

2.5. TUNEL staining

TUNEL (Roche, Germany) staining was performed using an in situ cell death detection kit according to the manufacturer's protocol. DAPI (Sigma, USA) staining was used to identify the cells in the field, and the labeled podocytes were analyzed by confocal microscopy (FV300; Olympus, Japan). The percentage of apoptotic cells was determined by counting the number of apoptotic TUNEL-positive cells (out of a total of more than 200 cells over five random fields) and dividing by the total number of cells.

2.6. Annexin V and propidium iodide staining assay

An AnnexinV/PI apoptosis detection kit (Beijing Biosea Biotechnology Co., Ltd., China) was used to stain Annexin V and Propidium Iodide according to the manufacturer's instructions. The cell pellets were resuspended in binding buffer and then treated with 10 μl of Annexin V for 15 min followed by the addition of 5 μl of Propidium iodide (PI) for 5 min in the dark. The rate of apoptosis was analyzed by flow cytometry (BD Biosciences, USA) using CellQuest software.

2.7. Measurement of intracellular ROS

The peroxide-sensitive fluorescent probe 2′, 7′-dichlorodihydrofluorescin diacetate (DCF-DA; Sigma) was used to measure intracellular ROS accumulation. The podocytes were first incubated for 45 min at 37 °C in PBS containing 10 μM DCF-DA to label intracellular ROS, and then the cells were washed. DCF fluorescence was detected by confocal microscopy as described above.

2.8. RhoA activation assay

RhoA activity was measured using a Rho activation assay kit (Cytoskeleton) according to manufacturer's instructions. The cells were lysed in cell lysis buffer and clarified by centrifugation. The supernatants were incubated with Rhotekin-Rho binding domain (RBD) glutathione affinity beads, which specifically bind to GTP-bound RhoA. The beads were washed, and the immunoprecipitated complex was resuspended in 2× Laemmli sample buffer and subjected to 15% SDS–PAGE, followed by Western blot analysis. Total RhoA protein was determined in separate Western blots and used to normalize GTP-bound RhoA densitometric units.

2.9. Statistical analysis

Data are presented as the mean ± SEM, with the number (n) of experiments indicated. Statistical analyses were performed using the unpaired t-test (SPSS 16.0), and graphs were prepared with Adobe Photoshop or plotted in Graphpad prism 5 (GraphPad Software, Inc.). $p < 0.05$ was considered significant.

3. Results

3.1. High glucose levels selectively increases the expression levels of TRPC6 mRNA and protein

We quantified the effects of high glucose levels on the expression levels of TRPC1, TRPC5, and TRPC6 mRNA and protein. In contrast with the control condition of 5.6 mmol/L glucose, the administration of 30 mmol/L glucose for 48 h significantly increased the TRPC6 mRNA levels and protein expression by 118% and 72%, respectively ($p < 0.01$; $n = 3$; Fig. 1A and D). However, this treatment did not lead to increases in TRPC1 or TRPC5 expression ($p > 0.05$; $n = 3$); on the contrary, TRPC5 mRNA levels were significantly decreased by high glucose levels (Fig. 1A) although the TRPC5 protein expression was not altered (Fig. 1D). Excluding osmotic effects, the administration of 30 mmol/L mannitol (instead of glucose) did not significantly affect the expression levels of TRPC6 mRNA or protein, (Fig. 1B and E). Furthermore, the effects of high glucose levels on TRPC6 expression were dose-dependent (Fig. 1B and E); significant increases in the expression levels TRPC6 mRNA and protein occurred at 20 mmol/L of glucose, with further increases at 30 mmol/L (Fig. 1B and E). High glucose levels also displayed a time-dependent effect on TRPC6 expression, as shown in Fig. 1C and F.

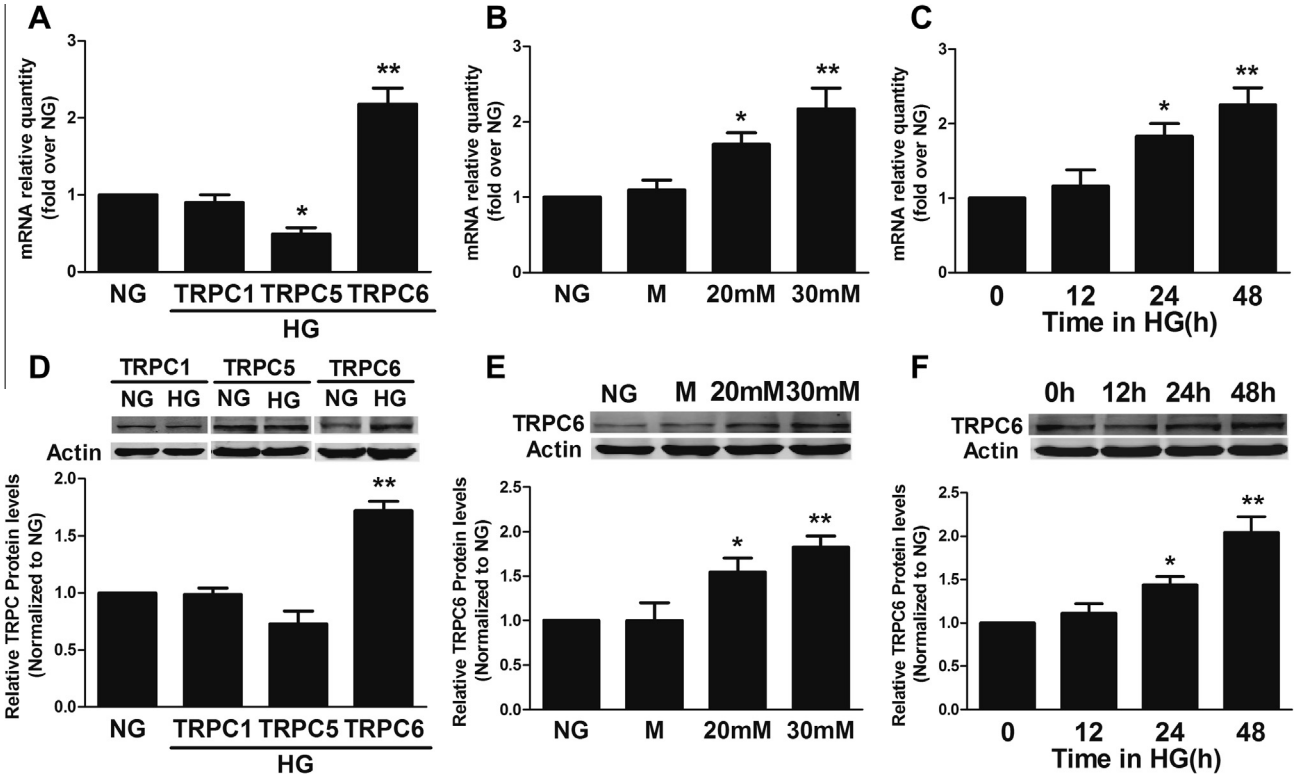

Fig. 1. The influence of high glucose concentration on TRPC6 mRNA levels and protein expression. Podocytes were treated with normal glucose (NG, 5.6 mmol/L) or high glucose (HG, 30 mmol/L) for 48 h. (A) The effects of HG on the mRNA levels of TRPC1, TRPC5, and TRPC6 ($n = 3$). A dose-dependent (B) and a time-dependent (C) increase in TRPC6 mRNA levels was observed in response to high glucose concentration ($n = 3$). (D) The effects of HG on the protein levels of TRPC1, TRPC5, and TRPC6 ($n = 3$). High glucose concentration increased TRPC6 protein levels in a dose-dependent (E) and a time-dependent (F) manner ($n = 3$). Administration of 30 mmol/L mannitol (M) did not significantly affect TRPC6 mRNA and protein expression (Fig. 1B and E). Asterisks indicate the statistical significance ($^{*}p < 0.05$, $^{**}p < 0.01$), with respect to NG.

3.2. High glucose levels enhance the TRPC6-dependent Ca^{2+} influx

It is well known that DAG can activate TRPC6 and result in Ca^{2+} entry via ROCE. Therefore, we tested the effect of high glucose levels on Ca^{2+} entry induced by 1-oleoyl-2-acetyl-sn-glycerol (OAG), a membrane-permeable DAG analogue. Internal Ca^{2+} stores were first depleted by incubating the podocytes with 1 μM TG for 5 min in a Ca^{2+}-free solution. The addition of 1.8 mM Ca^{2+} to the bathing solution induced a remarkable increase in $[Ca^{2+}]i$ (Fig. 2A). Following TG-induced SOCE, the application of 100 μM OAG induced an additional and substantial elevation of $[Ca^{2+}]i$ under conditions in which Ca^{2+} stores are already depleted (Fig. 2A). Therefore, OAG-induced Ca^{2+} influx was facilitated by plasmalemmal channels other than, or at least in addition to, SOCE. Note that the podocytes exhibited no spontaneous alterations in $[Ca^{2+}]i$ levels during these experiments, and the re-addition of extracellular Ca^{2+} in the absence of agonists had no effect on $[Ca^{2+}]i$ (data not shown). OAG-induced ROCE was significantly inhibited by treatment with 100 μM of the nonselective TRPC channel blocker 2-aminoethoxydiphenyl borate (2-APB; Fig. 2A). In lieu of selective pharmacological blockers of TRPC6, siRNA knockdown was used to determine whether OAG-induced Ca^{2+} influx requires TRPC6 function. The specificity and efficiency of TRPC6-siRNA was confirmed by real-time RT-PCR and Western blot analyses (Fig. 2B). Transfection with TRPC6 siRNA significantly reduced OAG-induced Ca^{2+} influx by 50% in contrast with transfection with scrambled siRNA ($p < 0.01$, $n = 3$; Fig. 2C). However, TG-induced SOCE was unaffected ($p > 0.05$, $n = 3$). Transfection with scrambled siRNA did not alter TG-induced SOCE or OAG-induced ROCE in contrast with the non-transfected control (data not shown). Taken together, these results strongly suggest that OAG-induced Ca^{2+} influx is TRPC6-dependent. Furthermore, the administration of 30 mmol/L of glucose for 48 h significantly increased OAG-induced ROCE by 115% ($p < 0.01$; $n = 3$; Fig. 2D), whereas this treatment had no effect on TG-induced SOCE ($p > 0.05$; $n = 3$). These results suggest that high glucose levels enhance TRPC6-dependent Ca^{2+} influx.

3.3. Blockage of TRPC6 activity attenuates high glucose-induced apoptosis

To investigate the role of TRPC6 in apoptosis induced by high glucose levels, we employed siRNA interference to assess the effect of TRPC6 depletion on high glucose-induced apoptosis using the TUNEL method and flow cytometry. The administration of 30 mmol/L glucose for 48 h caused a significant increase in the number of apoptotic cells in contrast with control glucose levels ($p < 0.01$; $n = 5$; Fig. 3A). Flow cytometry measurements further indicated the apoptotic rate was significantly increased in the high glucose group in contrast with the normal glucose group (Fig. 3B). Mannitol treatment had no effect on podocyte apoptosis as assessed using these two methods (data not shown). However, this increase in both the number of apoptotic cells and the apoptotic rate induced by high glucose levels was significantly inhibited by transfection with TRPC6 siRNA (Fig. 3), in contrast with non-transfected cells and cells transfected with scrambled siRNA. These data suggest the involvement of TRPC6 in high glucose-induced apoptosis.

3.4. High glucose-induced ROS generation mediates TRPC6 expression and Ca^{2+} influx

Given that the intracellular ROS level is elevated in high glucose-treated podocytes, we examined whether ROS are implicated

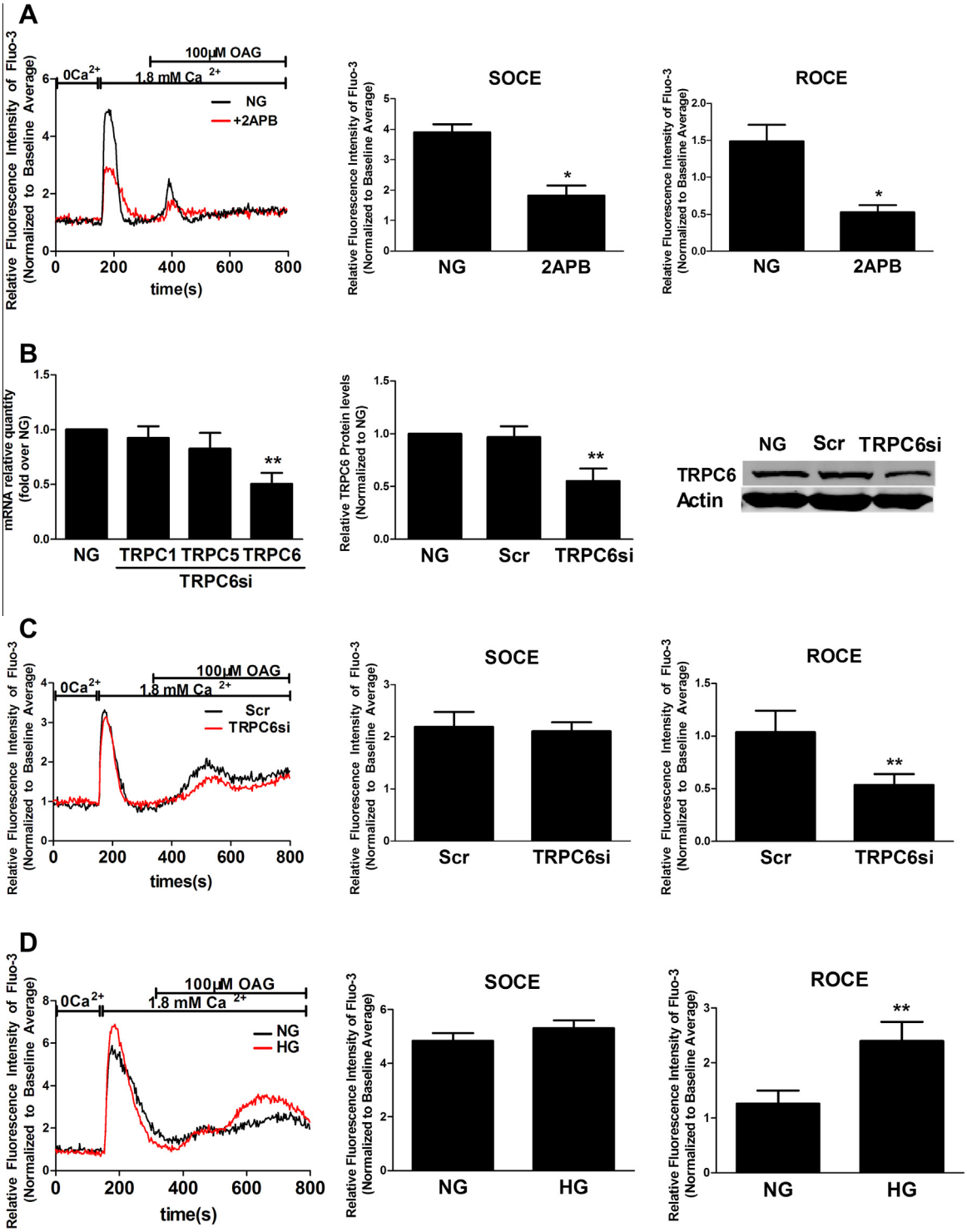

Fig. 2. Effects of TRPC6 knockdown and high glucose concentration on TG-induced SOCE and OAG-induced ROCE. (A) Representative traces (left) and summary data (right) showing that pretreatment with 100 μM 2-APB inhibited TG-induced SOCE and OAG-induced ROCE, respectively ($^{*}p < 0.05$ vs. NG, $n = 3$). (B) Real-time PCR experiments indicate that the TRPC6 siRNA significantly reduced the mRNA expression of TRPC6 ($^{**}p < 0.01$ vs. NG, $n = 3$) but not TRPC1 and TRPC5 ($p > 0.05$, $n = 3$). Western blot analyses reveal that transfection with TRPC6 siRNA significantly reduced TRPC6 protein expression compared to transfection with scrambled siRNA ($^{**}p < 0.01$, $n = 3$). (C) Representative traces (left) and summary data (right) indicate that transfection with TRPC6 siRNA significantly inhibited OAG-induced ROCE compared with transfection with scrambled siRNA ($^{**}p < 0.01$, $n = 3$), whereas TG-induced SOCE was unaffected ($p > 0.05$, $n = 3$). (D) Representative traces (left) and summary data (right) show that high glucose concentration enhanced OAG-induced ROCE ($^{**}p < 0.01$ vs. NG, $n = 3$) but did not affect TG-induced SOCE ($p > 0.05$, $n = 3$).

in the high glucose-induced TRPC6 upregulation. ROS induction by high glucose levels was investigated using the dye DCF-DA; in contrast with the control conditions, the administration of 30 mmol/L glucose for 48 h significantly increased the production of ROS ($p < 0.01$; $n = 6$; Fig. 4A). In addition, the concurrent administration of 10 mmol/L of the ROS inhibitor N-acetyl-L-cysteine (NAC) inhibited the effect of high glucose levels ($p < 0.01$; $n = 6$; Fig. 4A) and pretreatment with NAC attenuated the increased TRPC6 protein expression induced by high glucose levels ($p < 0.01$; $n = 3$; Fig. 4B). Consistent with this finding, TRPC6-dependent Ca^{2+} influx

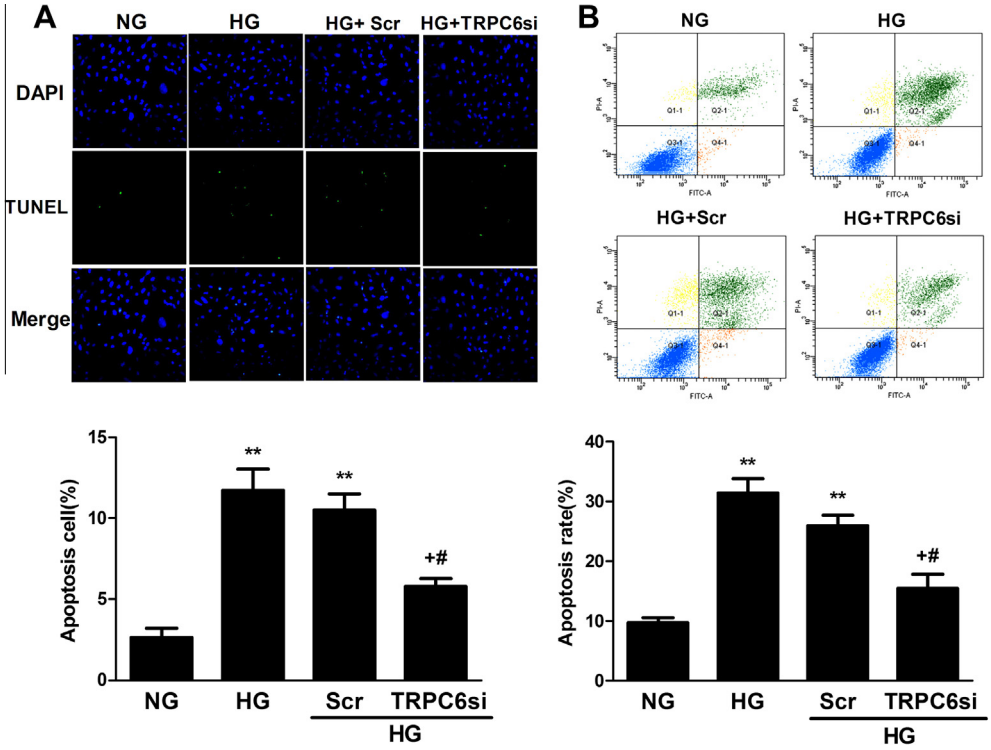

Fig. 3. High glucose-induced apoptosis was attenuated by depletion of TRPC6. Podocytes were transfected without or with TRPC6 siRNA (TRPC6si) or scrambled siRNA (Scr) followed by treatment with NG or HG for 48 h. (A) Apoptosis was determined using the TUNEL method, the results are expressed as apoptotic cell number (%) ($n = 5$). (B) Apoptosis was confirmed using flow cytometry, the results are expressed as apoptotic rate (%) including the early and late apoptosis rate ($n = 3$). $^{**}p < 0.01$ vs. NG; $^{+}p < 0.01$ vs. HG; $^{\#}p < 0.05$ vs. HG + Scr.

induced by high glucose levels was also inhibited by pretreatment with NAC (Fig. 4D). To further confirm the activation of TRPC6 by ROS, we examined the effects of exogenous H_2O_2 (500 μM) on TRPC6 protein expression and Ca^{2+} influx. As shown in Fig. 4C and E, H_2O_2 recapitulated the high glucose response, resulting in an increase in TRPC6 protein levels and Ca^{2+} influx ($p < 0.01$; $n = 4$, $p < 0.01$, $n = 3$, respectively). These data strongly suggest that the high glucose-associated ROS generation leads to increased TRPC6 expression and Ca^{2+} influx.

3.5. TRPC6 participates in high glucose-induced apoptosis via a RhoA dependent mechanism

RhoA activity was measured by an affinity pull-down assay using the GST fusion protein rhotekin that only recognizes the active form of RhoA (GTP-RhoA). Treatment with high glucose levels for 48 h caused a significant increase in RhoA activity in contrast with normal glucose levels ($p < 0.01$; $n = 3$; Supplementary Fig. 1A). This effect may be attributed to the high glucose-induced TRPC6 activation because transfection with TRPC6 siRNA attenuated the high glucose-induced increase in RhoA activity (Supplementary Fig. 1A), in contrast with non-transfected cells or cells transfected with the scrambled siRNA ($p < 0.01$; $n = 3$). Mannitol treatment had no effect on RhoA activity (data not shown). If the RhoA/ROCK pathway is activated by the TRPC6-dependent Ca^{2+} influx in high glucose-induced apoptosis, the inhibition of this downstream pathway should attenuate the high glucose effect. We measured the effect of Y27632, a selective ROCK inhibitor, on the high glucose-induced apoptosis and found the increase in both the number of apoptotic cells and the apoptotic rate induced by high glucose was significantly inhibited by the concurrent administration of Y27632 (10 μM; Supplementary Fig. 1B and C). These data suggest the involvement of the RhoA/ROCK pathway in TRPC6-dependent Ca^{2+} influx during high glucose-induced apoptosis.

4. Discussion

We have demonstrated that TRPC6 channels are involved in high glucose-induced apoptosis in podocytes. This finding is also supported by a recent clinical observation showing increased podocyte TRPC6 expression in kidney biopsies from four patients with DN [21]. As both gain-of-function mutations of the TRPC6 gene and elevated levels of wild-type TRPC6 protein result in glomerulosclerosis [7,8], altered TRPC6 channel activity may account for both podocyte apoptosis at the early stages of DN and for the pathogenesis of glomerulosclerosis at the later stages of DN.

A previous study in heterologous systems reported the TRPC6 channels can be activated by ROS, including H_2O_2 [12]. In podocytes, TRPC6 channels are also activated by endogenous ROS generated from insulin and puromycin aminonucleoside (PAN) treatments [22,23]. High glucose concentrations can also induce ROS generation [3,4]; however, it was not known whether high glucose concentrations can activate TRPC6. Our data reveal that high glucose-induced ROS increases TRPC6 expression and activity, consistent with previous studies. High glucose-induced ROS is at least partially generated through the stimulation of NADPH oxidases [3,4], particularly the Nox1 and Nox4 subforms. The expression levels of these subforms are increased by high glucose levels [3]. We did not investigate which of these NADPH oxidase subforms is responsible for the high glucose-induced TRPC6 activation in podocytes. However, it is possible that Nox4 may contribute to TRPC6 activation induced by high glucose levels because Nox4 is a crucial component of the pathway by which insulin and PAN can regulate TRPC6 activity [22,23]. It is interesting to note that there were no changes in NADPH oxidase-dependent ROS genera-

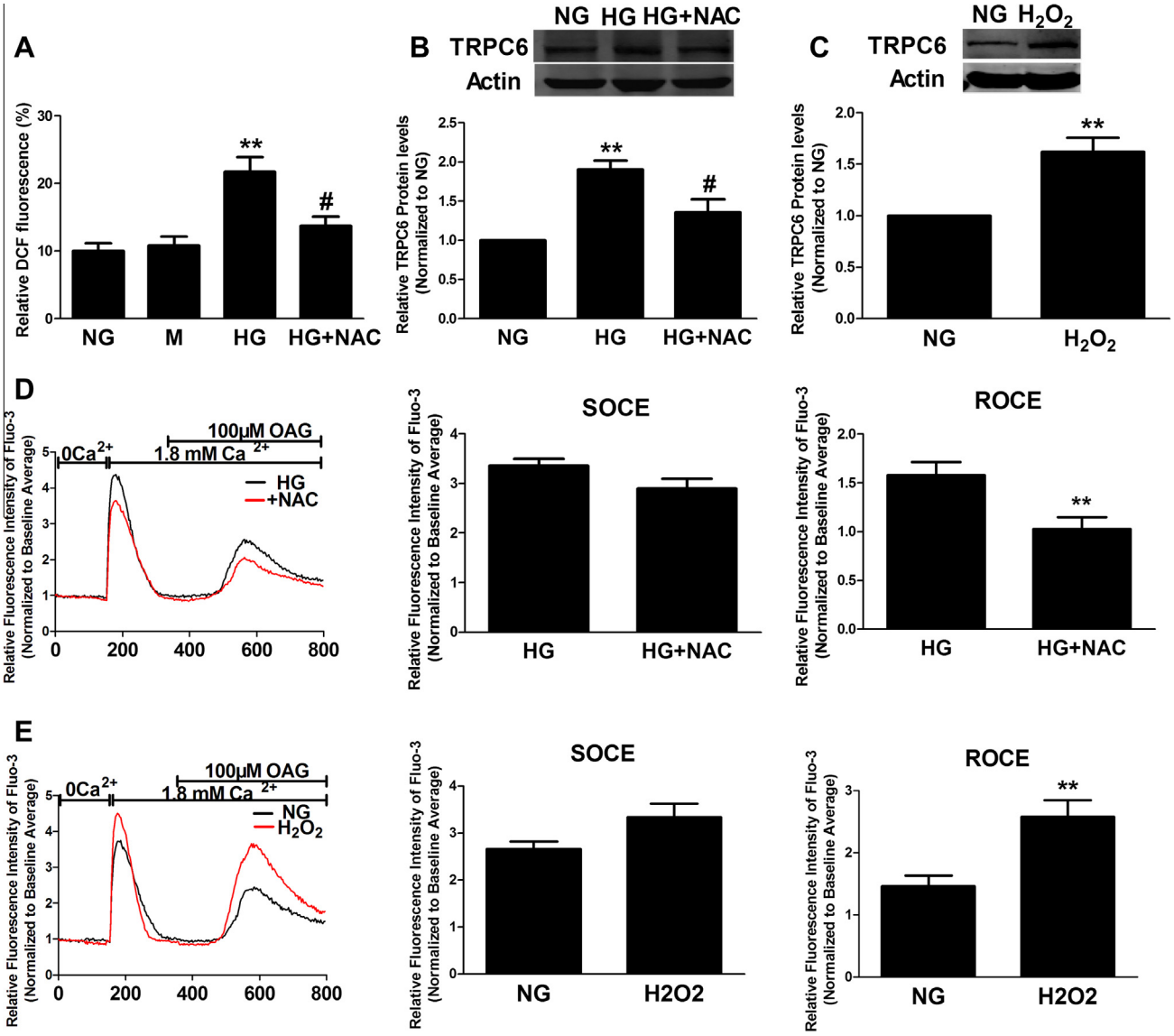

Fig. 4. ROS production induced by high glucose concentration mediated TRPC6 expression and Ca^{2+} influx. (A) High glucose concentration resulted in increased ROS generation. Podocytes were treated with NG, 30 mmol/L mannitol (M), HG, or HG + 10 mmol/L NAC, a ROS inhibitor, for 48 h ($n = 6$). (B) The increase in TRPC6 protein expression induced by the presence of high glucose was prevented by the pretreatment with 10 mmol/L NAC ($n = 3$). (C) Applying 500 μM H_2O_2 to podocytes for 2 h caused a significant increase in TRPC6 protein expression ($n = 4$). (D) The TRPC6-dependent Ca^{2+} influx induced by high glucose was also inhibited by pretreatment with NAC ($n = 3$). (E) Pretreatment of podocytes with 500 μM H_2O_2 led to a significant increase in OAG-induced ROCE ($n = 3$). $^{**}p < 0.01$ vs. NG or control; $^{\#}p < 0.05$ vs. HG.

tion upon acute exposure (6 h) of podocytes to high glucose levels [3]. Therefore, it is possible that the transient elevation of glucose levels observed in normal subjects following a glucose load may not activate the TRPC6 channels; a sustained exposure to high glucose levels may be required, as is found in the early stages of DN. A study using animal models demonstrated that TRPC6-deficient mice lack an overt renal phenotype [24], and another study suggested that in addition to ROS, high glucose levels induce TRPC6 activation via a Wnt/β-catenin signaling pathway [25].

Taken together, these findings suggest there is a common mechanism by which TRPC6-dependent Ca^{2+} influx contributes to the apoptosis processes that are induced by high glucose levels. A previous study indicated that two distinct signaling microdomains occur in podocytes: TRPC6 specifically interacts with and activates RhoA, and TRPC5 specifically interacts with and activates Rac1 [13]. In addition, another recent study found that NMDA receptor-evoked TRPC6 activation also increased RhoA activity [11]. Consistent with these results, we report that high glucose treatment also evoked a marked activation of RhoA; this effect was abolished by the knockdown of TRPC6 using siRNA, suggesting that RhoA is a downstream effector of TRPC6 activation. One recent study observed that RhoA/ROCK1 mediates high glucose-induced ROS generation and thereby promotes mitochondrial fission and podocyte apoptosis [5]. However, the activation mechanism of RhoA signaling has not yet been elucidated. Our results indicate that TRPC6-dependent Ca^{2+} influx may account for the high glucose-induced RhoA activation. Moreover, these results support a pathophysiological positive feedback loop in which high glucose-evoked ROS leads to TRPC6 and RhoA activation. This feedback loop could result in additional elevations in ROS and thereby promote podocyte apoptosis, although further investigation is needed to systematically test this model. It is important to note that our data do not exclude the possible model that the effect of TRPC6 channels on high glucose-induced podocyte apoptosis may be mediated, at least in part, through RhoA/ROCK-independent pathways. For example, high glucose-induced podocyte apoptosis requires

activation of calcineurin [26], which is also a downstream effector of the TRPC6 channel [14].

Acknowledgments

This work was supported by the National Nature Science Foundation of China (31071016) and the Nature Science Foundation of Heilongjiang Province (LC2009C03).

Appendix A. Supplementary data

Supplementary data associated with this article can be found, in the online version, at http://dx.doi.org/10.1016/j.bbrc.2013.03.087.

References

[1] M.E. Pagtalunan, P.L. Miller, S. Jumping-Eagle, R.G. Nelson, B.D. Myers, H.G. Rennke, N.S. Coplon, L. Sun, T.W. Meyer, Podocyte loss and progressive glomerular injury in type II diabetes, J. Clin. Invest. 99 (1997) 342–348.
[2] T.W. Meyer, P.H. Bennett, R.G. Nelson, Podocyte number predicts long-term urinary albumin excretion in Pima Indians with Type II diabetes and microalbuminuria, Diabetologia 42 (1999) 1341–1344.
[3] A.A. Eid, Y. Gorin, B.M. Fagg, R. Maalouf, J.L. Barnes, K. Block, H.E. Abboud, Mechanisms of podocyte injury in diabetes: role of cytochrome P450 and NADPH oxidases, Diabetes 58 (2009) 1201–1211.
[4] K. Susztak, A.C. Raff, M. Schiffer, E.P. Bottinger, Glucose-induced reactive oxygen species cause apoptosis of podocytes and podocyte depletion at the onset of diabetic nephropathy, Diabetes 55 (2006) 225–233.
[5] W. Wang, Y. Wang, J. Long, J. Wang, S.B. Haudek, P. Overbeek, B.H. Chang, P.T. Schumacker, F.R. Danesh, Mitochondrial fission triggered by hyperglycemia is mediated by ROCK1 activation in podocytes and endothelial cells, Cell Metab. 15 (2012) 186–200.
[6] S.E. Dryer, J. Reiser, TRPC6 channels and their binding partners in podocytes: role in glomerular filtration and pathophysiology, Am. J. Physiol. Renal Physiol. 299 (2010) F689–F701.
[7] J. Reiser, K.R. Polu, C.C. Moller, P. Kenlan, M.M. Altintas, C. Wei, C. Faul, S. Herbert, I. Villegas, C. Avila-Casado, M. McGee, H. Sugimoto, D. Brown, R. Kalluri, P. Mundel, P.L. Smith, D.E. Clapham, M.R. Pollak, TRPC6 is a glomerular slit diaphragm-associated channel required for normal renal function, Nat. Genet. 37 (2005) 739–744.
[8] C.C. Moller, C. Wei, M.M. Altintas, J. Li, A. Greka, T. Ohse, J.W. Pippin, M.P. Rastaldi, S. Wawersik, S. Schiavi, A. Henger, M. Kretzler, S.J. Shankland, J. Reiser, Induction of TRPC6 channel in acquired forms of proteinuric kidney disease, J. Am. Soc. Nephrol. 18 (2007) 29–36.
[9] T. Hofmann, A.G. Obukhov, M. Schaefer, C. Harteneck, T. Gudermann, G. Schultz, Direct activation of human TRPC6 and TRPC3 channels by diacylglycerol, Nature 397 (1999) 259–263.
[10] P.F. Worley, W. Zeng, G.N. Huang, J.P. Yuan, J.Y. Kim, M.G. Lee, S. Muallem, TRPC channels as STIM1-regulated store-operated channels, Cell Calcium 42 (2007) 205–211.
[11] E.Y. Kim, M. Anderson, S.E. Dryer, Sustained activation of N-methyl-D-aspartate receptors in podoctyes leads to oxidative stress, mobilization of transient receptor potential canonical 6 channels, nuclear factor of activated T cells activation, and apoptotic cell death, Mol. Pharmacol. 82 (2012) 728–737.
[12] S. Graham, M. Ding, Y. Ding, S. Sours-Brothers, R. Luchowski, Z. Gryczynski, T. Yorio, H. Ma, R. Ma, Canonical transient receptor potential 6 (TRPC6), a redox-regulated cation channel, J. Biol. Chem. 285 (2010) 23466–23476.
[13] D. Tian, S.M. Jacobo, D. Billing, A. Rozkalne, S.D. Gage, T. Anagnostou, H. Pavenstaedt, H.H. Hsu, J. Schlondorff, A. Ramos, A. Greka, Antagonistic regulation of actin dynamics and cell motility by TRPC5 and TRPC6 channels, Sci. Signal. 3 (2010) ra77.
[14] A. Greka, P. Mundel, Balancing calcium signals through TRPC5 and TRPC6 in podocytes, J. Am. Soc. Nephrol. 22 (2011) 1969–1980.
[15] L. Zhu, R. Jiang, L. Aoudjit, N. Jones, T. Takano, Activation of RhoA in podocytes induces focal segmental glomerulosclerosis, J. Am. Soc. Nephrol. 22 (2011) 1621–1630.
[16] L. Wang, M.J. Ellis, J.A. Gomez, W. Eisner, W. Fennell, D.N. Howell, P. Ruiz, T.A. Fields, R.F. Spurney, Mechanisms of the proteinuria induced by Rho GTPases, Kidney Int. 81 (2012) 1075–1085.
[17] H. Zhang, J. Ding, Q. Fan, S. Liu, TRPC6 up-regulation in Ang II-induced podocyte apoptosis might result from ERK activation and NF-kappaB translocation, Exp. Biol. Med. (Maywood) 234 (2009) 1029–1036.
[18] S. Chen, F.F. He, H. Wang, Z. Fang, N. Shao, X.J. Tian, J.S. Liu, Z.H. Zhu, Y.M. Wang, S. Wang, K. Huang, C. Zhang, Calcium entry via TRPC6 mediates albumin overload-induced endoplasmic reticulum stress and apoptosis in podocytes, Cell Calcium 50 (2011) 523–529.
[19] R. Zhang, H. Sun, C. Liao, H. Yang, B. Zhao, J. Tian, S. Dong, Z. Zhang, J. Jiao, Chronic hypoxia in cultured human podocytes inhibits BKCa channels by upregulating its beta4-subunit, Biochem. Biophys. Res. Commun. 420 (2012) 505–510.
[20] C. Liao, H. Yang, R. Zhang, H. Sun, B. Zhao, C. Gao, F. Zhu, J. Jiao, The upregulation of TRPC6 contributes to Ca(2)(+) signaling and actin assembly in human mesangial cells after chronic hypoxia, Biochem. Biophys. Res. Commun. 421 (2012) 750–756.
[21] F. Thilo, Y. Liu, C. Loddenkemper, R. Schuelein, A. Schmidt, Z. Yan, Z. Zhu, A. Zakrzewicz, M. Gollasch, M. Tepel, VEGF regulates TRPC6 channels in podocytes, Nephrol. Dial. Transplant. 27 (2012) 921–929.
[22] E.Y. Kim, M. Anderson, S.E. Dryer, Insulin increases surface expression of TRPC6 channels in podocytes: role of NADPH oxidases and reactive oxygen species, Am. J. Physiol. Renal Physiol. 302 (2012) F298–F307.
[23] Z. Wang, X. Wei, Y. Zhang, X. Ma, B. Li, S. Zhang, P. Du, X. Zhang, F. Yi, NADPH oxidase-derived ROS contributes to upregulation of TRPC6 expression in puromycin aminonucleoside-induced podocyte injury, Cell. Physiol. Biochem. 24 (2009) 619–626.
[24] A. Dietrich, Y.S. Mederos, M. Gollasch, V. Gross, U. Storch, G. Dubrovska, M. Obst, E. Yildirim, B. Salanova, H. Kalwa, K. Essin, O. Pinkenburg, F.C. Luft, T. Gudermann, L. Birnbaumer, Increased vascular smooth muscle contractility in TRPC6−/− mice, Mol. Cell Biol. 25 (2005) 6980–6989.
[25] Z. Li, J. Xu, P. Xu, S. Liu, Z. Yang, Wnt/beta-catenin signalling pathway mediates high glucose induced cell injury through activation of TRPC6 in podocytes, Cell Prolif. 46 (2013) 76–85.
[26] L. Wang, J.H. Chang, S.Y. Paik, Y. Tang, W. Eisner, R.F. Spurney, Calcineurin (CN) activation promotes apoptosis of glomerular podocytes both in vitro and in vivo, Mol. Endocrinol. 25 (2011) 1376–1386.